



Physicochemical and structural characteristics of chitosan nanopowders prepared by ultrafine milling

Wei Zhang^a, Jiali Zhang^b, Qixing Jiang^a, Wenshui Xia^{a,*}

^a State Key Laboratory of Food Science and Technology, School of Food Science and Technology, Jiangnan University, Wuxi, Jiangsu 214122, China

^b School of Medicine and Pharmaceutics, Jiangnan University, Wuxi, Jiangsu 214122, China

ARTICLE INFO

Article history:

Received 5 April 2011

Received in revised form 19 July 2011

Accepted 26 July 2011

Available online 3 August 2011

Keywords:

Chitosan

Ultrafine milling

Nanopowder

ABSTRACT

Two different molecular weights of chitosan were pulverized to nanopowders by ultrafine milling. The nanopowders were characterized by viscometry small angle X-ray scattering (SAXS), transmission electron microscopy (TEM), X-ray diffraction (XRD), thermogravimetric analysis (TGA), FT-IR spectroscopy and UV–vis spectroscopy. Our results showed that ultrafine milling effectively reduced the particle size of chitosan to a nanoscale. The viscosity average molecular weight (M_v) of chitosan was decreased by the milling treatment. The crystalline structure of chitosan was destroyed by the milling since the nanopowder exhibited an amorphous XRD pattern. In addition, thermal stability of the low molecular weight chitosan was decreased after the milling treatment. FT-IR and UV–vis spectra showed that the milling process did not cause significant changes in the chemical structure of chitosan.

© 2011 Elsevier Ltd. All rights reserved.

1. Introduction

Chitosan, is a natural cationic polysaccharide, obtained by the alkaline, partial deacetylation of chitin, which originates from shells of crustaceans. Due to the unique polycationic nature, chitosan has been proposed for various applications in food, pharmaceutical and chemical industries (Kumar, 2000).

Nanotechnology is an emerging technology that holds great promises for the future. Nanosizing gives materials new characteristics as a result of surface and small size/quantum effects. Chitosan nanoparticles have been extensively explored for pharmaceutical applications, as carriers for drug, gene and vaccine delivery (Dev et al., 2010; Yang, Yuan, Cai, Wang, & Zong, 2009; Zheng et al., 2007). Furthermore, chitosan nanoparticles have been shown to have effective antitumor activity (Qi & Xu, 2006; Qi, Xu, & Chen, 2007) and hypocholesterolemic activity (Tao et al., 2011; Zhang, Tao, Guo, Hu, & Su, 2011).

Chitosan nanoparticles are generally prepared ionotropic gelation, self-assembling or microemulsion methods (Agnihotri, Mallikarjuna, & Aminabhavi, 2004). The microemulsion method can produce nanoparticles with narrow size distribution, but large quantities of organic solvent must be used (Mitra, Gaur, Ghosh, & Maitra, 2001). Though self-assembling is a simple method, must be modified by introducing new chemical groups (Yinsong, Lingrong, Jian, & Zhang, 2007). Ionotropic gelation offers a mild preparation

method in the aqueous environment, without the introduction of chemical groups into chitosan molecules. For this method, the size of nanoparticles is affected by the concentration and molecular weight of chitosan, and nanoparticle concentration must be kept at low level to avoid flocculation (Gan, Wang, Cochrane, & McCarron, 2005). Besides, the chitosan nanoparticle suspension is a thermodynamically unstable system, and particle size changes during storage (López-León, Carvalho, Seijo, Ortega-Vinuesa, & Bastos-Gonzalez, 2005). Tao et al. (2011) and Zhang et al. (2011) prepared chitosan nanoparticles by ionotropic gelation, and then spray-dried the nanoparticle suspension to produce a nanopowder to facilitate the application and storage of nanoparticles.

Ultrafine milling is an effective method to produce a nanopowder (Zhu, Huang, Peng, Qian, & Zhou, 2010). Nevertheless, there are no studies reported on producing chitosan nanopowders by ultrafine milling. The aim of this study, therefore, was to explore the possibility of directly preparing chitosan nanopowders by ultrafine milling, followed by investigation of the physicochemical and structural properties of the chitosan nanopowders.

2. Materials and methods

2.1. Materials

High molecular weight chitosan (HMWC) was obtained from Nantong Shuanglin Biotechnology Co., Ltd. (Jiangsu, China). Sodium hydroxide, sodium chloride, acetic acid, and 30% (w/w) hydrogen peroxide aqueous solution, analytical purity, were supplied by Sinopharm Chemical Reagent Co., Ltd. (Shanghai, China).

* Corresponding author. Tel.: +86 510 85919121; fax: +86 510 85919121.

E-mail address: xiaws@jiangnan.edu.cn (W. Xia).

2.2. The preparation of low molecular weight chitosan (LMWC)

HMWC powder was completely dissolved in 1% (w/v) acetate acid solution to make a solution of 2% (w/v). Thirty percent (w/v) H₂O₂ aqueous solution was added in the solution by 1:100 (v/v). After reaction at 60 °C for 1.5 h, the solution was adjusted to pH 8. The precipitated chitosan was recovered by centrifugation and washed to pH 7 with deionized water. The chitosan paste was frozen and thawed to separate the water, and then dried at 60 °C.

2.3. Ultrafine milling of chitosan

Chitosan was milled with TJH-2-4L multidimensional swing high-energy nano-ball-mill (Qinghuangdao Taiji Ring Nano-Products Co., Ltd., Hebei, China), with a driving motor of 7 kW. Chitosan powder (80 g) and ZrO₂ balls (6–10 mm in diameter) were mixed in a volume ratio of 1:2 in a 4000 ml strengthened stainless steel grinding bowl. Experiments were carried out in a dry mode for 12 h without any milling aid. The temperature was maintained at 30 °C by cold water recirculation. The obtained powders were sealed in aluminum foil for storage. The milling products of HMWC and LMWC were denoted by the abbreviations HMWC-NP and LMWC-NP, respectively.

2.4. Determination of molecular weight

The molecular weight of chitosan was measured in a solvent of 0.2 M NaCl/0.1 M CH₃COOH at 25 °C using an Ubbelohde viscometer, as described by No, Park, Lee, and Meyers (2002). The viscosity average molecular weight (*M_v*) was calculated using the Mark–Houwink equation: $[\eta] = k(M_v)^\alpha$, where *k* and α were $1.81 \times 10^{-3} \text{ cm}^3 \text{ g}^{-1}$ and 0.93, respectively. Each measurement was carried out in triplicate.

2.5. Particle size determination

The particle size distribution of original chitosan powder was determined using Mastersizer 2000 (Malvern Instrument Co., UK). Before measuring, chitosan powder was ultrasonically dispersed in water for 1 min.

The particle size distribution of chitosan nanopowder was determined according to the China National Standard GB/T 13321 (2004). Nanopowder was dispersed in celloidin–acetone solution, and acetone was removed by drying the mixture at 20–50 °C. The sample was analyzed by small angle X-ray scattering (SAXS) (Rigaku-3014, Rigaku, Japan) under the following conditions: Cu-K α radiation, 35 kV, 20 mA and measurement range 2θ 0–3°.

2.6. Electron microscopy

Morphological characterization of particles in original chitosan powder was performed using a scanning electron microscope (Quanta-200 SEM, FEI, Netherlands). The sample was coated with spraying gold powder to make it conductive.

A transmitting electron microscope (TEM) was employed to image the particles of nanopowder. The nanopowder was suspended in water for 3 min sonication to obtain a dilute suspension. A drop of dilute suspension was deposited onto a glow discharged carbon-coated microscopy grid and allowed to dry. The sample was observed by using Hitachi H-7000 TEM (Japan).

2.7. X-ray diffraction (XRD)

The X-ray diffraction patterns of the chitosan samples were measured using a Bruker AXS D8 Advance diffractometer

(Germany) under the following conditions: Cu-K α radiation, 40 kV, 40 mA and measurement range 2θ 4–40°.

2.8. Thermogravimetric analysis (TGA)

TGA was performed on a Mettler Toledo TGA/SDTA851 Thermo gravimeter (Mettler Toledo Corp., Zurich, Switzerland) with STARE software (version 9.01) was used to analyze the thermal stability of the samples. Samples were heated from 30 to 500 °C at a heating rate of 10 °C/min under N₂ at 30 ml/min during the analysis.

2.9. FT-IR spectroscopy

Fourier transform infrared (FT-IR) spectrum was recorded on a Nicolet Nexus 470 instrument (Nicolet Instrument, Thermo Company, Madison, USA). Samples were prepared as KBr pellet and scanned against a blank KBr pellet background at wave number range 4000–400 cm^{−1} with resolution of 4.0 cm^{−1}.

2.10. UV–vis spectroscopy

0.1 g of chitosan was dissolved in 50 ml 1% (w/v) HCl solution. After complete dissolution, the solution was centrifuged at 3000 × *g* for 10 min to remove the insoluble material. UV–vis absorption spectra were obtained using a UV1000 spectrophotometer (Tech-comp Ltd., China) in the range of 200–500 nm.

2.11. Statistical analysis

The test data were statistically analyzed using DPS 7.05 for windows (Zhejiang University, Hangzhou, China). Duncan's multiple range test were used to determine the difference among means at the level of 0.05.

3. Results and discussion

3.1. Molecular weight

The *M_v* of HMWC, LMWC and the milling products (HMWC-NP and LMWC-NP) are listed in Table 1. As Table 1 shows, the milling process decreased the *M_v* of chitosan. It was suggested that chitosan molecules were degraded during the process of milling. This finding was similar with some previous studies concerning starches, which reported that molecular degradation occurred during ball-milling of starches (Huang, Xie, Chen, Lu, & Tong, 2008; Tamaki, Hisamatsu, Teranishi, & Yamada, 1997). The *M_v* of HMWC-NP and LMWC-NP was decreased by 52.93% and 18.02% compared with the original samples, respectively. This result indicated that high molecular weight chitosan was more susceptible to damage during ball milling.

3.2. Particle size distribution and morphology

Fig. 1a shows the particle size distributions of HMWC and LMWC powders. The particle size of HMWC was distributed in a range from 2 μm to 700 μm and mostly concentrated in the range of

Table 1
Molecular weights of chitosan.

Original sample	<i>M_v</i> ^a (kDa)	
	Before milling	After milling
HMWC	766.77 ± 10.34 ^a	360.91 ± 6.18 ^b
LMWC	66.25 ± 1.25 ^a	54.31 ± 1.57 ^b

^a Values are means ± SD (*n* = 3). Means with different superscripts within a row indicate a significant differences (*P* < 0.05).

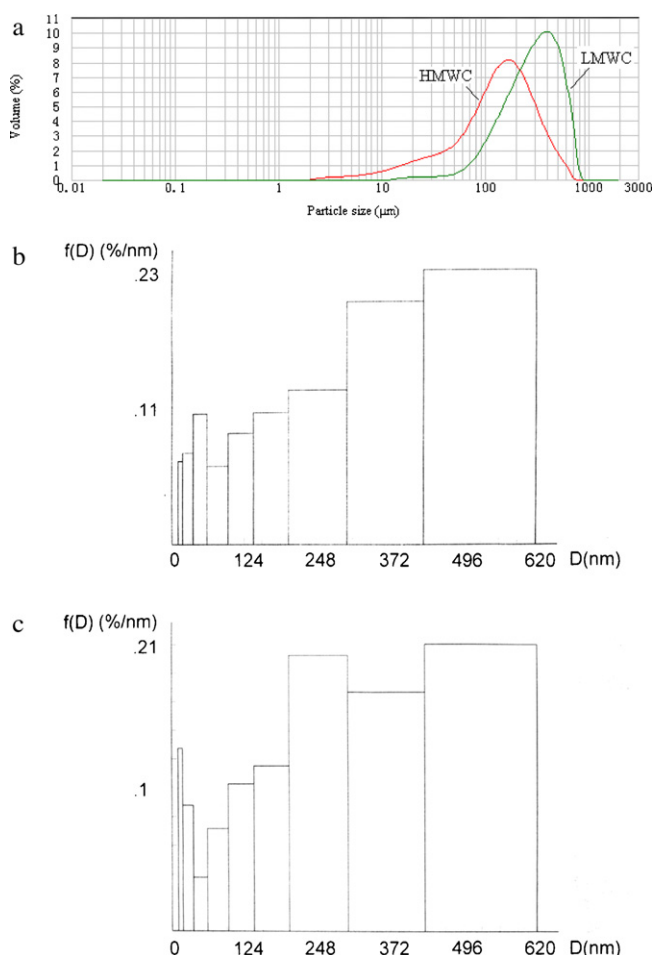


Fig. 1. The particle size distributions of chitosan powders. (a) HMWC and LMWC; (b) HMWC-NP; and (c) LMWC-NP.

60–400 μm with an average particle size of 167.1 μm . The particle size of LMWC was higher than that of HMWC, and its average particle size was about 325.6 μm . The difference of HMWC and LMWC in particle size might be resulted from their different preparation methods. As a commercial powder, HMWC was milled and sieved to make a fine powder. However, LMWC was prepared in our own laboratory, which was stored without further treatment after drying.

SEM micrographs of HMWC and LMWC powders are shown in Fig. 2a and b. The particles of HMWC were observed to be in the form of flakes, and there were large amounts of small particles distributing among large flakes. However, massive blocky particles were found in LMWC powder and less small particles were present compared with HMWC powder. The particle sizes of the two powders estimated from SEM images coincided with the results from the Mastersizer 2000.

SAXS technique is an effective method to determine the size distribution of nanopowder. Fig. 1b and c shows the particle size distributions of the two milling products. The average particle sizes of HMWC-NP and LMWC-NP were 375.2 and 359.5 nm, respectively. This demonstrated that particle sizes of the two milling products were in the nanoscale range and chitosan nanopowder could be prepared by ultrafine milling.

The morphologies of HMWC-NP and LMWC-NP nanopowders pictured by TEM are shown in Fig. 2c and d. The nanoparticles of HMWC-NP were round, and tended to agglomerate. For LMWC-NP, nanoparticles were irregular, and particles in TEM image were obscure, which might be due to the partial dissolution of chitosan

during TEM sample preparation. The solubility of chitosan in water was dependant on the molecular weight, and solubility could be improved by decreasing molecular weight (Mao et al., 2004). After milling, the molecular weight of chitosan was decreased, which might lead to an increase in the water-soluble fraction.

3.3. Crystalline structure

Previous literature revealed that at least six crystalline polymorphs had been found for chitosan, including 'tendon', 'annealed', '1-2', 'L-2', 'form I' and 'form II' (Cervera et al., 2004). Fig. 3 shows the X-ray diffraction patterns of chitosan samples. The XRD patterns of the HMWC and LMWC powders exhibited two characteristic peaks at 2θ of about 12° and 20° , which coincided with the 'L-2 polymorph' reported by Qin, Du, and Xiao (2002).

For the two nanopowders, halo diffraction patterns were observed, indicating an amorphous state of these powders. Thus, in the process of the milling, crystalline structure of chitosan was destroyed. This finding was similar with some previous studies concerning ball-milling of starch and cellulose, which reported that ball-milling treatment destroyed the crystalline structures of these two materials (Huang et al., 2008; Kocherbitov, Ulvenlund, Kober, Jarring, & Arnebrant, 2008).

3.4. TGA

The thermal properties of chitosan were characterized by TGA. As Fig. 4 shows, HMWC and HMWC-NP had similar curves, which showed a maximum degradation temperature (T_{max}) at about 300°C . This indicated that thermal stability of HMWC-NP was similar to that of HMWC. Thermal degradation behaviors of LMWC and LMWC-NP were different, and the T_{max} of these two samples were about 280°C and 260°C , respectively. It was suggested that thermal stability of LMWC-NP decreased compared with LMWC, which might be attributed to the decrease in molecular weight and the disruption of crystalline structure. For chitosan with low molecular weight, slight change in molecular weight and crystalline structure could cause significant alteration in thermal stability (Qin et al., 2002, 2003).

3.5. FT-IR and UV-vis spectra analysis

FT-IR spectra of chitosan are shown in Fig. 5. For the FT-IR spectrum of HMWC, the broad band at around 3436cm^{-1} was attributed to $-\text{NH}$ and $-\text{OH}$ stretching vibration, as well as inter- and extra-molecular hydrogen bonding of chitosan molecules. The characteristic absorption bands of HMWC appeared at 1644cm^{-1} (Amide I), 1594cm^{-1} ($-\text{NH}_2$ bending) and 1320cm^{-1} (Amide III) (Feng & Xia, 2011). It was found that the spectrum of LMWC was similar to that of HMWC. This suggested that the chemical degradation with peroxide hydrogen did not greatly change the chemical structure of chitosan, which was consistent with the previous literature (Qin et al., 2002). The nanopowders and the original powders did not show great differences in FT-IR spectra, which suggested that the ultrafine milling had no obvious effect on chemical structure of chitosan.

The UV-vis spectra of chitosan are shown in Fig. 6. Broad absorption bands between 250 and 300 nm were observed for the four samples. Based on the data reported in the published literature, the broad absorption band might be ascribed to $\text{C}=\text{O}$ group (Cai et al., 2010). It was observed that the absorption intensities of HMWC-NP and LMWC-NP in this zone increased compared with the original samples. This might be attributed to the degradation of chitosan molecules during milling. Degradation increased the terminals of chitosan, possibly resulting in the increase of $\text{C}=\text{O}$ groups. No special peaks were found in the spectra of HMWC-NP and LMWC-NP,

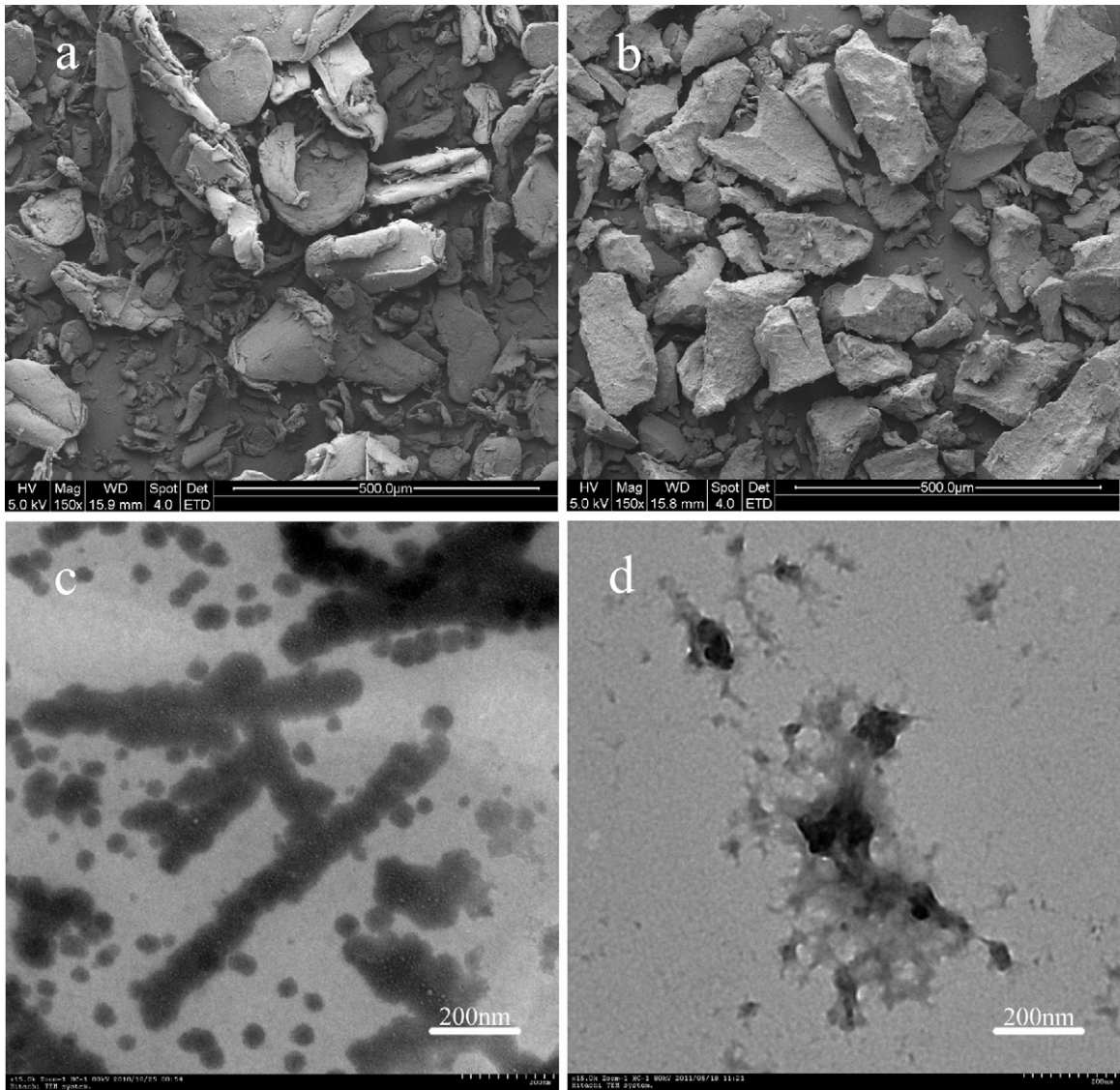


Fig. 2. SEM and TEM images of chitosan powders. (a) HMWC; (b) LMWC; (c) HMWC-NP; and (d) LMWC-NP.

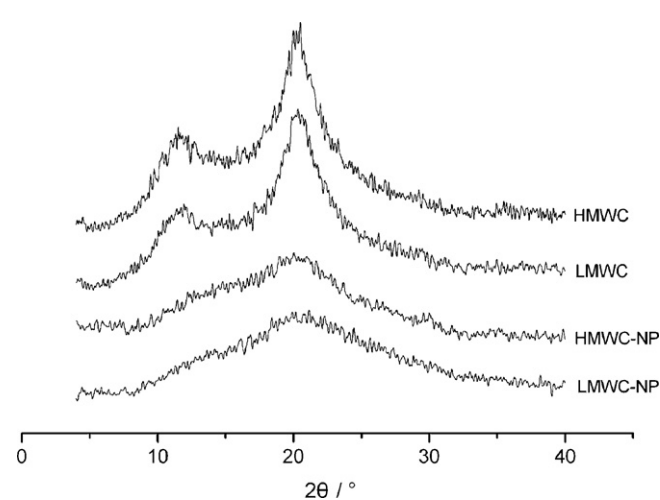


Fig. 3. XRD patterns of chitosan.

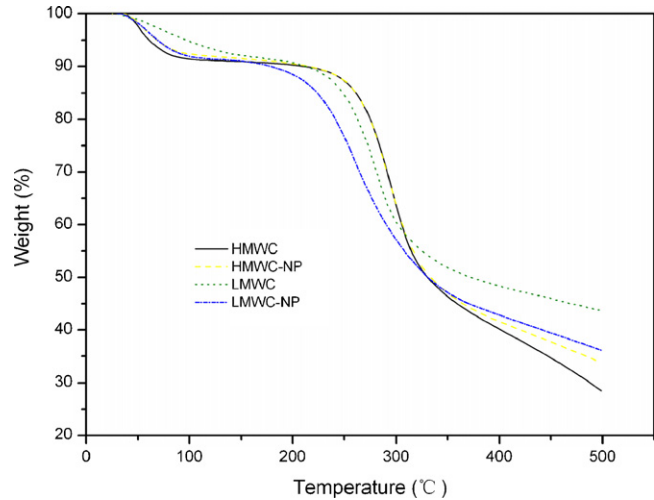


Fig. 4. TGA curves of chitosan.

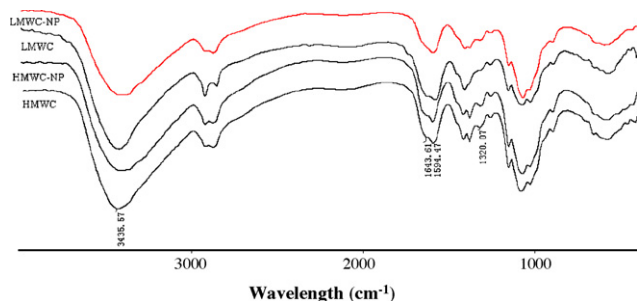


Fig. 5. FT-IR spectra of chitosan.

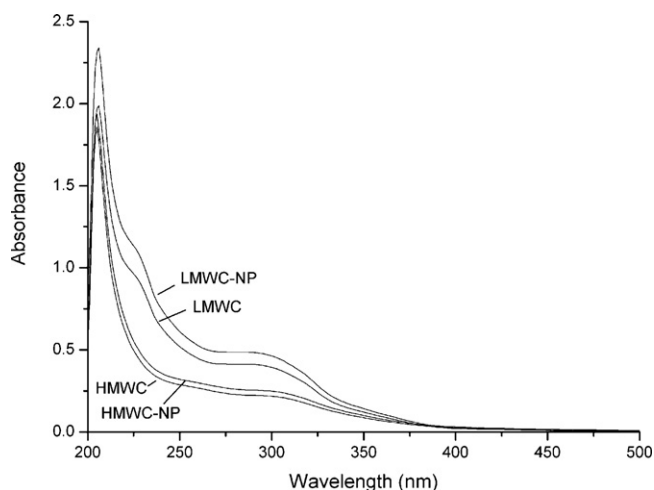


Fig. 6. UV-vis spectra of chitosan.

which further demonstrated that the treatment of ultrafine milling did not cause great changes in the chemical structure of chitosan.

4. Conclusion

Chitosan with molecular weights of 766.77 and 66.25 kDa were successfully pulverized to nanopowders by ultrafine milling. The average particle sizes of the two nanopowders were 375.2 and 359.5 nm, respectively. After ultrafine milling, molecular weights of the two samples were decreased and their crystalline structures were destroyed. The milling treatment decreased the thermal stability of the low molecular weight chitosan. FT-IR and UV-vis spectra revealed that the milling treatment did not cause great change in chemical structure of chitosan. These findings suggest that ultrafine milling is an effective method to prepare chitosan nanopowder and some physicochemical properties of chitosan will change during the preparation process, which may affect its application and deserve to be further researched.

Acknowledgements

This research was financially supported by the fund for 863 Project (nos. 2007AA100401 and 2011AA090801), the National Natural Science Funds of China (nos. 20876068 and 20571034), the Science and Technology Plan Project of Guangdong Province (no. 2010B090400467), the guidance project of State key Laboratory of Food Science and Technology (no. SKLF-MB-200805), and

the Fund Project for Transformation of Scientific and Technological Achievements of Jiangsu Province (BA2009082).

References

- Agnihotri, S. A., Mallikarjuna, N. N., & Aminabhavi, T. M. (2004). Recent advances on chitosan-based micro- and nanoparticles in drug delivery. *Journal of Controlled Release*, 100(1), 5–28.
- Cai, Q. Y., Gu, Z. M., Chen, Y., Han, W. Q., Fu, T. M., Song, H. C., et al. (2010). Degradation of chitosan by an electrochemical process. *Carbohydrate Polymers*, 79(3), 783–785.
- Cervera, M. F., Heinamaki, J., Rasanen, M., Maunu, S. L., Karjalainen, M., Acosta, O. M. N., et al. (2004). Solid-state characterization of chitosans derived from lobster chitin. *Carbohydrate Polymers*, 58(4), 401–408.
- Dev, A., Binulal, N. S., Anitha, A., Nair, S. V., Furukie, T., Tamura, H., et al. (2010). Preparation of poly(lactic acid)/chitosan nanoparticles for anti-HIV drug delivery applications. *Carbohydrate Polymers*, 80(3), 833–838.
- Feng, Y. W., & Xia, W. S. (2011). Preparation, characterization and antibacterial activity of water-soluble O-fumaryl-chitosan. *Carbohydrate Polymers*, 83(3), 1169–1173.
- Gan, Q., Wang, T., Cochrane, C., & McCarron, P. (2005). Modulation of surface charge, particle size and morphological properties of chitosan-TPP nanoparticles intended for gene delivery. *Colloids and Surfaces B-Biointerfaces*, 44(2–3), 65–73.
- GB/T 13321. (2004). Nanoscale powder determination of particle size distribution – small angle X-ray scattering method. Published 29.09.04, Implemented 01.04.05.
- Huang, Z. Q., Xie, X. L., Chen, Y., Lu, J. P., & Tong, Z. F. (2008). Ball-milling treatment effect on physicochemical properties and features for cassava and maize starches. *Comptes Rendus Chimie*, 11(1–2), 73–79.
- Kocherbitov, V., Ulvenlund, S., Kober, M., Jarring, K., & Arnebrant, T. (2008). Hydration of microcrystalline cellulose and milled cellulose studied by sorption calorimetry. *Journal of Physical Chemistry B*, 112(12), 3728–3734.
- Kumar, M. N. V. R. (2000). A review of chitin and chitosan applications. *Reactive and Functional Polymers*, 46(1), 1–27.
- López-León, T., Carvalho, E. L. S., Seijo, B., Ortega-Vinuesa, J. L., & Bastos-Gonzalez, D. (2005). Physicochemical characterization of chitosan nanoparticles: Electrokinetic and stability behavior. *Journal of Colloid and Interface Science*, 283(2), 344–351.
- Mao, S., Shuai, X., Unger, F., Simon, M., Bi, D., & Kissel, T. (2004). The depolymerization of chitosan: Effects on physicochemical and biological properties. *International Journal of Pharmaceutics*, 281(1–2), 45–54.
- Mitra, S., Gaur, U., Ghosh, P. C., & Maitra, A. N. (2001). Tumour targeted delivery of encapsulated dextran–doxorubicin conjugate using chitosan nanoparticles as carrier. *Journal of Controlled Release*, 74(1–3), 317–323.
- No, H. K., Park, N. Y., Lee, S. H., & Meyers, S. P. (2002). Antibacterial activity of chitosans and chitosan oligomers with different molecular weights. *International Journal of Food Microbiology*, 74(1–2), 65–72.
- Qi, L. F., & Xu, Z. R. (2006). In vivo antitumor activity of chitosan nanoparticles. *Bioorganic & Medicinal Chemistry Letters*, 16(16), 4243–4245.
- Qi, L. F., Xu, Z. R., & Chen, M. L. (2007). In vitro and in vivo suppression of hepatocellular carcinoma growth by chitosan nanoparticles. *European Journal of Cancer*, 43(1), 184–193.
- Qin, C. Q., Du, Y. M., & Xiao, L. (2002). Effect of hydrogen peroxide treatment on the molecular weight and structure of chitosan. *Polymer Degradation and Stability*, 76(2), 211–218.
- Qin, C., Du, Y., Zong, L., Zeng, F., Liu, Y., & Zhou, B. (2003). Effect of hemicellulase on the molecular weight and structure of chitosan. *Polymer Degradation and Stability*, 80(3), 435–441.
- Tamaki, S., Hisamatsu, M., Teranishi, K., & Yamada, T. (1997). Structural change of potato starch granules by ball-mill treatment. *Starch/Stärke*, 49, 431–488.
- Tao, Y., Zhang, H. L., Gao, B., Guo, J. A., Hu, Y. M., & Su, Z. Q. (2011). Water-soluble chitosan nanoparticles inhibit hypercholesterolemia induced by feeding a high-fat diet in male Sprague-Dawley rats. *Journal of Nanomaterials*, doi:10.1155/2011/814606
- Yang, X., Yuan, X., Cai, D., Wang, S., & Zong, L. (2009). Low molecular weight chitosan in DNA vaccine delivery via mucosa. *International Journal of Pharmaceutics*, 375(1–2), 123–132.
- Yinsong, W., Lingrong, L., Jian, W., & Zhang, Q. (2007). Preparation and characterization of self-aggregated nanoparticles of cholesterol-modified O-carboxymethyl chitosan conjugates. *Carbohydrate Polymers*, 69(3), 597–606.
- Zhang, H. L., Tao, Y., Guo, J., Hu, Y. M., & Su, Z. Q. (2011). Hypolipidemic effects of chitosan nanoparticles in hyperlipidemia rats induced by high fat diet. *International Immunopharmacology*, 11(4), 457–461.
- Zheng, F., Shi, X. W., Yang, G. F., Gong, L. L., Yuan, H. Y., Cui, Y. J., et al. (2007). Chitosan nanoparticle as gene therapy vector via gastrointestinal mucosa administration: Results of an in vitro and in vivo study. *Life Sciences*, 80(4), 388–396.
- Zhu, K., Huang, S., Peng, W., Qian, H., & Zhou, H. (2010). Effect of ultrafine grinding on hydration and antioxidant properties of wheat bran dietary fiber. *Food Research International*, 43(4), 943–948.